nature structural & molecular biology

Recognition of helical kinks by xeroderma pigmentosum group A protein triggers DNA excision repair

Ulrike Camenisch[1], Ramiro Dip[1], Sylvie Briand Schumacher[1], Benjamin Schuler[2] & Hanspeter Naegeli[1]

The function of human XPA protein, a key subunit of the nucleotide excision repair pathway, has been examined with site-directed substitutions in its putative DNA-binding cleft. After screening for repair activity in a host-cell reactivation assay, we analyzed mutants by comparing their affinities for different substrate architectures, including DNA junctions that provide a surrogate for distorted reaction intermediates, and by testing their ability to recruit the downstream endonuclease partner. Normal repair proficiency was retained when XPA mutations abolished only the simple interaction with linear DNA molecules. By contrast, results from a K141E K179E double mutant revealed that excision is crucially dependent on the assembly of XPA protein with a sharp bending angle in the DNA substrate. These findings show how an increased deformability of damaged sites, leading to helical kinks recognized by XPA, contributes to target selectivity in DNA repair.

Nucleotide excision repair (NER) is a versatile defense system that eliminates bulky DNA adducts generated by environmental genotoxic agents[1–3]. Cyclobutane dimers and (6-4) photoproducts, induced by UV light, are the most abundant substrates of this universal DNA-repair process under physiological conditions[4,5]. The importance of NER is demonstrated by the three inherited diseases xeroderma pigmentosum (XP), Cockayne syndrome and thrichothiodystrophy[6]. In particular, the XP syndrome represents a DNA-repair disorder leading to photosensitivity and a >2,000-fold increased incidence of skin cancer[7–9]. Individuals affected by XP are classified into seven repair-deficient complementation groups designated XP-A through XP-G, with associated proteins XPA through XPG[6].

NER activity is initiated by recognition of a bulky adduct followed by dual incision of damaged DNA, thereby releasing the offending lesion as part of a single-stranded oligonucleotide segment[10–12]. Two distinct pathways have been discerned in this excision response[13,14]. Global genome repair depends on XPC protein to eliminate bulky lesions throughout the genome, whereas transcription-coupled repair, mediated by Cockayne syndrome group A and B proteins, removes DNA lesions only from the transcribed strand of active genes. Common to both pathways is the sequential recruitment of TFIIH, XPG, replication protein A (RPA), XPA and XPF, together with excision repair cross complementing-1 (ERCC1), to damaged sites[15–18].

XPA protein is essential for DNA incision in both global genome repair and transcription-coupled repair, but the precise function of this core subunit has remained elusive. It is a zinc metalloprotein of 273 amino acid residues that forms homodimers[19] and also associates with other NER constituents. Separate interaction domains have been deduced from the analysis of deletion constructs (**Fig. 1a**). The N-terminal portion (residues 1–97) binds the 34-kDa subunit of RPA and to ERCC1 (refs. 20,21). The C-terminal domain (residues 226–273) interacts with TFIIH[22]. Its central domain (residues 98–219) constitutes the minimal polypeptide fragment for binding to DNA[23,24] and includes a motif (residues 153–176) that interacts with the 70-kDa subunit of RPA[21]. The NMR solution structure of this central domain has revealed a positively charged cleft with the appropriate dimensions to accommodate double-stranded DNA (**Fig. 1b**)[25,26]. The surface of this region displays a cluster of basic side chains (**Fig. 1c**) that may interact with the negatively charged phosphate moieties of the DNA backbone. Here, we have performed a systematic mutational analysis to understand how this substrate-recognition cleft of human XPA protein may regulate the multicomponent DNA-excision reaction.

RESULTS

DNA-repair activity of site-directed mutants

A host-cell reactivation assay was exploited to monitor the activity of repair factors in their endogenous context[27]. XP-A fibroblasts were transfected with a reporter system in conjunction with an expression vector (pcXPA) coding for human XPA protein or its mutants. The reporter construct, which carries a firefly luciferase gene, was damaged by UV irradiation and supplemented with an undamaged control vector that expresses the *Renilla reniformis* luciferase. After varying repair times, firefly luciferase activity was determined in cell lysates and normalized against the internal *Renilla* luciferase standard.

Owing to the repair defect of XP-A cells, expression of the reporter gene was suppressed when the vector was UV-irradiated. However, DNA repair and, hence, firefly luciferase production was restored after transfection with pcXPA, demonstrating that the genetic defect of XP-A fibroblasts is corrected by human XPA protein (**Fig. 2a**). In contrast, luciferase expression was not rescued when the same XP-A

[1]Institute of Pharmacology and Toxicology, University of Zürich-Vetsuisse, Winterthurerstrasse 260, CH-8057 Zürich, Switzerland. [2]Institute of Biochemistry, University of Zürich, Winterthurerstrasse 190, CH-8057 Zürich, Switzerland. Correspondence should be addressed to H.N. (naegelih@vetpharm.unizh.ch).

Received 7 October 2005; accepted 10 January 2006; published online 19 February 2006; doi:10.1038/nsmb1061

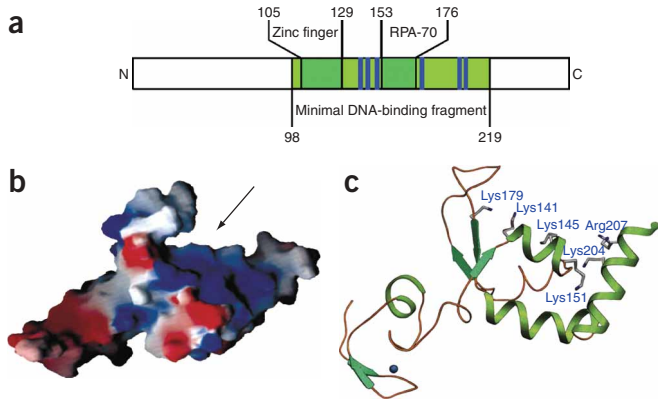

Figure 1 Structure of human XPA protein. (**a**) Minimal DNA-binding fragment[23]. Blue bars indicate positively charged residues. (**b**) Distribution of electrostatic potential on the surface of the central domain (adapted from ref. 25). Blue, positive; red, negative; arrow, DNA-binding cleft. (**c**) Solution structure of the minimal DNA-binding fragment[25]. Positively charged side chains are thought to mediate interactions with the nucleic acid backbone. These basic residues are evolutionary well conserved (**Supplementary Fig. 3** online).

cells were transfected with the empty pcDNA vector. The residual background activity observed in the presence of this vector alone was due to a fraction of reporter constructs lacking UV lesions in the luciferase sequence. No substantial increase of repair activity was detected when, instead of XPA, XPC protein was overexpressed in XP-A fibroblasts (**Fig. 2b**). Repair complementation was markedly reduced when the XPA sequence was modified to carry a termination codon at position 207 (R207stop), which is responsible for severe XP symptoms[24]. By contrast, a human polymorphic allele (R228Q), identified from phenotypically normal individuals[28], yielded full complementation (**Fig. 2b**), thus demonstrating the validity of our screening assay.

The DNA-repair capacity of each mutant is reported as the percentage of wild-type complementation after deduction of background luciferase expression determined with empty vector. First, the positively charged side chains of Lys141, Lys145, Lys151, Lys179, Lys204 and Arg207, located in the presumed DNA-binding cleft, were eliminated by converting these amino acids to glycine, but the repair activity was not significantly ($P < 0.05$) reduced by such single Lys→Gly or Arg→Gly substitutions (**Supplementary Fig. 1** online). More extreme substitutions were introduced by changing the same basic residues to the negatively charged glutamate. Again, none of these single Lys→Glu or Arg→Glu replacements diminished the DNA repair response significantly ($P < 0.05$; **Supplementary Fig. 1**). Next, pairs of adjacent lysine and arginine residues in the presumed DNA-binding cleft were changed to glutamate. A strong reduction of repair activity was conferred by simultaneous mutations at positions 141 and 179 (**Fig. 2c**). This tandem glutamate mutant showed the same poor repair performance as the R207stop allele from XP patients. Other substitutions of neighboring lysines (for example, K141E K145E or K145E K151E) decreased DNA repair to a more moderate extent. Glutamate substitutions of residues 167 and 168, located just outside the putative DNA-binding domain[26], resulted in marginal changes of repair activity (**Fig. 2c**).

Further experiments were performed to test all possible combinations of double glutamate mutations within the DNA-binding surface involving either position 141 or 179 (**Fig. 2d**). This systematic analysis confirmed that the most prominent repair defect is associated with the K141E K179E mutant, whereas all other tandem mutations caused less severe effects. The repair-deficient protein was generated by converting two positively charged side chains into negatively charged ones. When the same two lysines were changed to the neutral glycine residue instead of glutamate, the repair activity of the resulting mutant (K141G K179G) was restored nearly to the wild-type level (**Fig. 2e**).

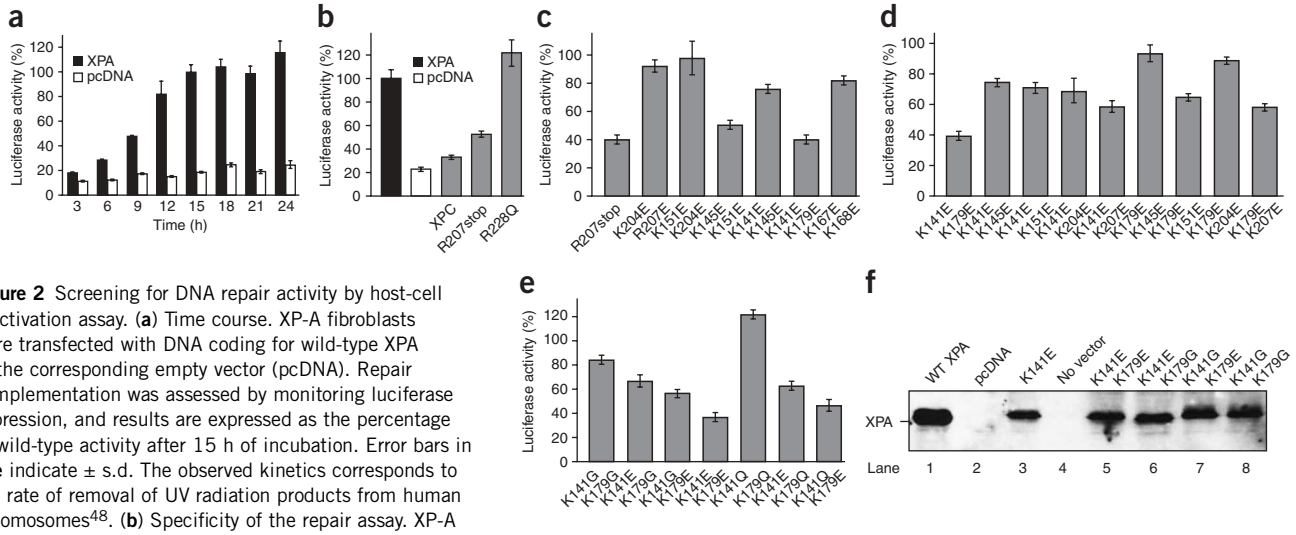

Figure 2 Screening for DNA repair activity by host-cell reactivation assay. (**a**) Time course. XP-A fibroblasts were transfected with DNA coding for wild-type XPA or the corresponding empty vector (pcDNA). Repair complementation was assessed by monitoring luciferase expression, and results are expressed as the percentage of wild-type activity after 15 h of incubation. Error bars in **a**–**e** indicate ± s.d. The observed kinetics corresponds to the rate of removal of UV radiation products from human chromosomes[48]. (**b**) Specificity of the repair assay. XP-A fibroblasts were transfected with the wild-type XPA sequence, empty control vector (pcDNA) or vectors containing the sequence of human XPC protein, a repair-deficient XPA mutant (R207stop) or a polymorphic XPA allele (R228Q). (**c**) DNA repair activity after introduction of double glutamate mutations at neighboring lysine or arginine residues in the DNA-binding cleft. Results are expressed as the percentages of wild-type complementation after deduction of background activity obtained with empty vector. (**d**) Effects of combinations of double mutations involving Lys141 or Lys179. (**e**) Different effects of glycine, glutamine and glutamate mutations at position 141 or 179. (**f**) Expression of mutant proteins in XPA-fibroblasts. Soluble cell lysates (10 μg) were analyzed by western blotting with a monoclonal antibody to human XPA. WT denotes wild-type. Lane 2, XP-A fibroblasts transfected with empty vector. Lane 4, untransfected cells.

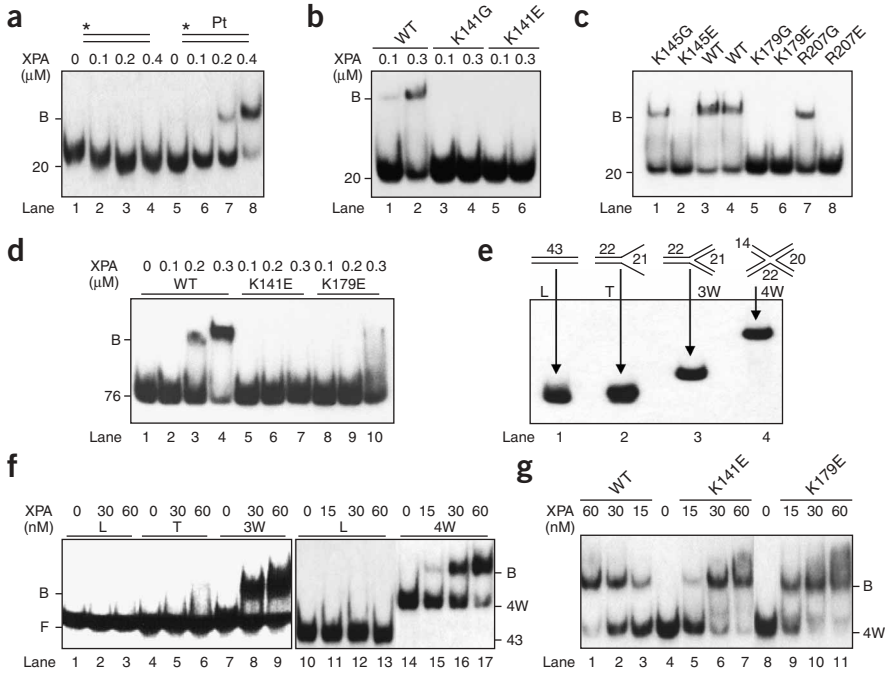

Figure 3 DNA-binding properties of XPA mutants. (**a**) Preference of wild-type (WT) XPA for damaged DNA. XPA protein was incubated with undamaged (lanes 1–4) or cisplatin-damaged 20-mer duplexes (lanes 5–8). The formation of nucleoprotein complexes was monitored on nondenaturing polyacrylamide gels. The positions of free (20) and bound (B) DNA fragments are indicated. (**b**) Comparison between wild-type XPA and position 141 mutants. (**c**) Comparison between wild-type XPA (in duplicate, lanes 3 and 4) and position 145, 179 and 207 mutants. All proteins were tested at a concentration of 0.3 μM. (**d**) Control experiment with single-stranded DNA of 76 residues. (**e**) Analysis of structurally distinct DNA substrates on a nondenaturing 10% polyacrylamide gel. Lane 1, linear 43-mer duplex (L). Lane 2, transition molecule composed of a 22-bp arm with 21-nt overhangs (T). Lane 3, three-way junction (3W). Lane 4, four-way junction (4W). (**f**) EMSA demonstrating the preference of wild-type XPA protein for three-way junctions (lanes 7–9) and four-way junctions (lanes 14–17), relative to linear DNA (lanes 1–3 and 10–13) or transition substrates (lanes 4–6). (**g**) Normal interaction of K141E and K179E single mutants with four-way junctions.

In contrast, when one position was converted to glutamate and the other site was changed to glycine, the resulting K141G K179E and K141E K179G mutants showed an intermediate loss of activity. The same two residues were also replaced by glutamine, which has approximately the same size as glutamate but carries no electrostatic charge. The double glutamine mutant (K141Q K179Q) showed normal repair activity, whereas the mixed K141E K179Q and K141Q K179E substitutions yielded intermediate effects (**Fig. 2e**). An immunoblot analysis of transfected XP-A fibroblasts demonstrated that the repair-deficient tandem mutant K141E K179E (**Fig. 2f**, lane 5) was expressed in similar amounts to the repair-proficient K141E (lane 3) and K141G K179G variants (lane 8).

Structure-specific DNA binding

Wild-type and mutant XPA proteins were produced in *Escherichia coli* and purified to homogeneity (**Supplementary Fig. 2** online) for use in a series of DNA-binding assays. Initially, electrophoretic mobility shift assays (EMSAs) were used to examine affinities of these proteins for radiolabeled 20-base-pair (bp) duplexes containing a single intrastrand 1,2-d(GpG) cisplatin cross-link[23,29,30]. As expected, XPA protein showed a marked preference for the platinated duplexes relative to undamaged controls of the same length and sequence (**Fig. 3a**), but this interaction was disrupted by a single glycine or glutamate mutation at position 141 (**Fig. 3b**) or 179 (**Fig. 3c**, lanes 5 and 6). At position 145, DNA binding was abolished by a Lys→Glu substitution but not by a glycine replacement (**Fig. 3c**, lanes 1 and 2). At position 207, only the glycine mutation resulted in retention of DNA-binding capacity (**Fig. 3c**, lanes 7 and 8). XPA protein also binds single-stranded oligonucleotides, but this interaction was disrupted by K141E and K179E substitutions (**Fig. 3d**). Thus, several amino acid replacements in the positively charged cleft of XPA protein perturb its DNA binding in reconstitution assays. However, all these single XPA mutants elicited normal repair activity, implying that the simple association with single-stranded or double-stranded linear probes does not reflect the true function of this NER subunit.

We next tested whether XPA protein may be specialized for the recognition of an unusual DNA architecture that arises during the assembly of excision complexes. Y-shaped junction molecules, each consisting of a 22-bp duplex with two 21-nucleotide (nt) single-stranded extensions (**Fig. 3e**), were constructed to reproduce the sites of helical conversion from double-stranded to single-stranded DNA generated as a consequence of local unwinding. Radiolabeled three- and four-way junctions composed of double-helical stems ranging from 14 to 22 bp (**Fig. 3e**) were constructed to mimic the DNA deformations, involving sharp backbone kinks, encountered when multiprotein complexes assemble on DNA[31]. To our surprise, we found that XPA protein binds more effectively to three-way junctions (**Fig. 3f**, lanes 7–9) and four-way junctions (lanes 14–17) than to transition substrates (lanes 4–6) or linear 43-bp controls (lanes 1–3 and 10–13). Furthermore, the Lys→Glu single mutants at position 141 or 179, which did not interact with linear DNA, were able to bind four-way junctions with an affinity identical to that of wild-type protein (**Fig. 3g**). These results indicate that the helical kinks of such artificially distorted substrates may constitute a more representative probe than linear DNA to monitor the function of XPA protein.

Association of tandem XPA mutants with kinked DNA

The K141E K179E double mutant was purified for examination of the molecular basis of its repair defect. Lys141 is positioned at the beginning of a short α-helix and Lys179 precedes a β-strand (**Fig. 1c**). An analysis of the modified amino acid sequence by the PredictProtein program[32] predicted that glutamate substitutions at these sites would be compatible with both structural features. In fact, EMSAs showed that the purified K141E K179E double mutant binds four-way junctions with exactly the same affinity as wild-type XPA (**Fig. 4a**). However, this tandem derivative generated different nucleoprotein products (denoted B1) that migrate faster than the control complexes (B2). A super-shift assay using antibodies to human XPA confirmed that the tandem mutant itself is responsible for the formation of these aberrant complexes (**Fig. 4b**). As shown for the

respective single mutants (**Fig. 3**), the composite K141E K179E derivative rejected linear double-stranded (**Fig. 4c**) or linear single-stranded DNA (**Fig. 4d**) as binding partners. The lack of interaction of this K141E K179E mutant with single-stranded DNA rules out the possibility that the increased mobility of the products that it forms with kinked substrates may arise from an association with just the radiolabeled DNA strand. Further analysis by CD revealed that the tandem mutant has the same amount of secondary structure as wild-type XPA, confirming that the native protein fold is not disrupted (**Fig. 4e**). Other tandem mutants, which showed nearly normal DNA repair activity, generated either wild-type nucleoprotein complexes (data not shown) or, as in the case of K179E K204E, a mixture of wild-type (B2) and aberrant (B1) products upon incubation with four-way DNA (**Fig. 4f**, lanes 6–9). To summarize, it seems that the interaction of XPA protein with the kinked backbone of the four-way DNA junction correlates with the biological function of this repair subunit.

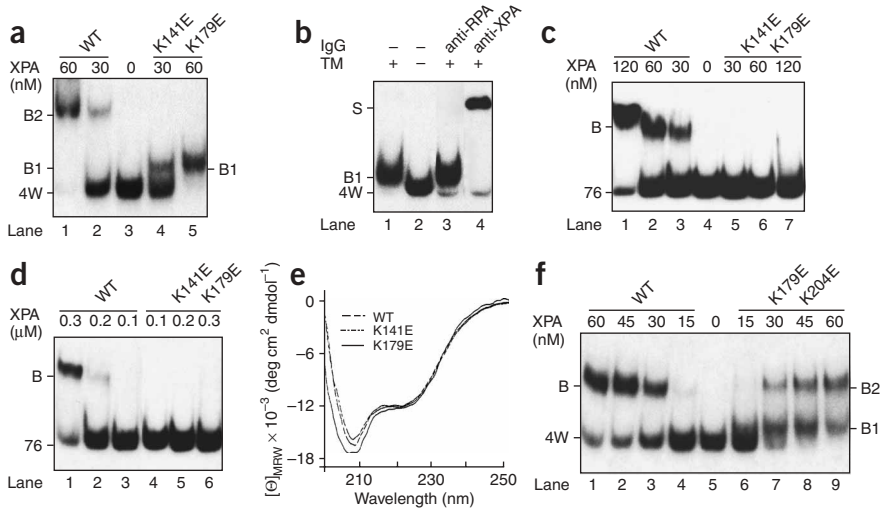

Figure 4 DNA-binding profiles of XPA tandem mutants. (**a**) Comparison of nucleoprotein complexes formed by wild-type (WT) XPA (lanes 1 and 2) and the K141E K179E mutant (lanes 4 and 5) using four-way junction substrates. Lane 3, no protein added to the reaction. (**b**) The specificity of complexes formed by the K141E K179E tandem mutant (TM, 60 nM) is demonstrated by the addition of mouse monoclonal antibodies (1 μg) against human XPA (lane 4). S, super-shifted products; 4W, four-way junction. Lane 3, control incubation with antibodies (1 μg) against the 32-kDa subunit of human RPA. (**c**) Inability of the K141E K179E mutant to associate with linear double-stranded DNA of 76 bp. The 76-mer duplex contains an identical number of nucleotides as the four-way junction. (**d**) Inability of the K141E K179E mutant to associate with linear single-stranded DNA of 76 nt. (**e**) Far-UV CD spectra of wild-type protein (two independent fractions) and the K141E K179E mutant. (**f**) Comparison of nucleoprotein complexes formed by wild-type XPA and the K179E K204E tandem mutant.

Photo–cross-linking to kinked DNA

We next examined the binding of XPA proteins to four-way junctions using a photo–cross-linking assay. A photoreactive azido-base analog was placed in the center of the radiolabeled 43-mer strand of the four-way substrate (**Fig. 5a**). After preincubation of these probes with XPA protein, the mixtures were UV-irradiated and the covalent protein–DNA complexes were visualized on denaturing polyacrylamide gels. A specifically cross-linked product with an expected mass of >50 kDa was generated when the samples were exposed to UV light in the presence of XPA protein at concentrations of 30 nM or higher (**Fig. 5b**). This UV-dependent reactivity toward four-way junctions was substantially reduced by the introduction of a Lys→Glu mutation at position 141 or 179 (**Fig. 5c**). Also, the K141E K179E tandem mutant was completely refractory to cross-linking with the central region of the four-way junction (**Fig. 5d**, lanes 6–9), revealing a key role of Lys141 and Lys179 in mediating the interaction of XPA protein with the site of kinked DNA.

Recruitment of the XPF–ERCC1 heterodimer

XPA protein is required for the incorporation of the XPF–ERCC1 heterodimer into growing NER complexes[18,33]. We therefore tested whether the distinct nucleoprotein structures formed by wild-type XPA and the K141E K179E derivative differ in their ability to recruit the XPF-ERCC1 endonuclease. To avoid degradation of the DNA substrate, a mutant form of XPF was used that contains an inactivating catalytic-site substitution (K716A)[34]. At the low concentration tested, the XPF–ERCC1 complex did not interact with the DNA substrate (**Fig. 6a**, lane 2). However, prior association of wild-type XPA protein with the four-way substrate generated nucleoprotein intermediates (lane 3) that were able to recruit the XPF–ERCC1 nuclease, giving rise to complexes of higher molecular weight (lane 4). These products (B3) contained both XPA and XPF–ERCC1, because their mobility was decreased not only relative to the intermediates formed by XPA alone (B2) but also relative to the complexes induced with higher amounts of XPF–ERCC1 (data not shown). In contrast to the action of normal XPA, the aberrant nucleoprotein intermediates generated by the K141E K179E mutant (lane 5) were impaired in their ability to recruit the XPF–ERCC1 nuclease (lane 6).

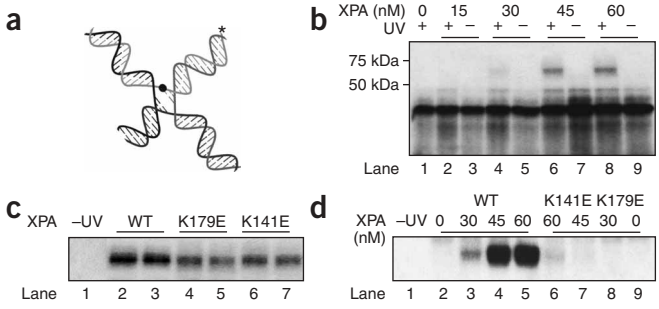

Figure 5 Photo–cross-linking to the kinked junction region. (**a**) Position of the photoreactive azido moiety (dot) in the radiolabeled strand (asterisk) of the four-way DNA junction. (**b**) Sodium dodecyl sulfate gel analysis of covalent complexes resulting from irradiation of reaction mixtures containing wild-type XPA and the photoreactive four-way junction. Lane 1, control sample with UV-irradiated substrate alone. (**c**) Covalent complexes formed by incubating wild-type protein (lanes 2 and 3) or the K141E and K179E single mutants (lanes 4–7) with the photoreactive four-way junction. Protein concentrations were 60 nM. Lane 1, unirradiated control reaction with wild-type XPA. (**d**) The K141E K179E tandem mutant (lanes 6–9) is not cross-linked to the junction region. Lane 1, unirradiated control reaction containing 60 nM of wild-type protein.

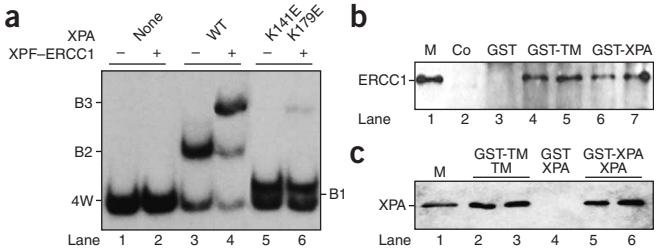

Figure 6 Recruitment of XPF–ERCC1 and dimerization. (**a**) Four-way DNA junctions were preincubated with 30 nM of wild-type XPA (lanes 3 and 4) or the K141E K179E tandem mutant (lanes 5 and 6). After 15 min, the reactions of lanes 4 and 6 were supplemented with XPF–ERCC1 (3 nM). After another 15 min, the mixtures were resolved on nondenaturing polyacrylamide gels. Lane 1, control reaction without protein. Lane 2, reaction with XPF–ERCC1 (3 nM) alone. (**b**) Interaction between ERCC1 and the K141E K179E tandem mutant. Pull-down assays were performed by coincubating 10 nM each of histidine-tagged ERCC1–XPF and GST fusion proteins with either wild-type XPA (GST-XPA, lanes 6 and 7) or the K141E K179E tandem mutant (GST-TM, lanes 4 and 5). Pull-downs were analyzed by western blotting with antibodies to histidine. Lane 1, purified ERCC1 marker (M). Lane 2, control reaction without GST fusion (Co). Lane 3, control reaction with naked GST. (**c**) Homodimerization of XPA proteins. Pull-down assays were performed by coincubating 10 nM each of histidine- and GST-tagged wild-type XPA (lanes 5 and 6) or of histidine- and GST-tagged K141E K179E mutant (lanes 2 and 3). Lane 1, purified XPA marker. Lane 4, control reaction with naked GST protein.

The XPA domain required for interaction with ERCC1 is located outside the DNA-binding motif[21]. Accordingly, pull-down experiments using XPA protein fused to glutathione-*S*-transferase (GST) demonstrated that the association with ERCC1 remains intact despite the tandem K141E K179E mutation (**Fig. 6b**, lanes 4 and 5). Similarly, we determined using XPA-GST fusion proteins that the formation of XPA homodimers is not disturbed by the double K141E K179E replacement (**Fig. 6c**, lanes 2 and 3). These interaction analyses show that the K141E K179E substitutions alter the DNA-binding properties without perturbing the molecular function of other XPA domains.

DISCUSSION

None of the few naturally occurring point mutations in XP-A patients map to the presumed DNA-binding cleft[24] and, to our knowledge, only an R207G mutant has been tested before, with conflicting results[35,36]. Therefore, the goal of this study was to analyze the role of this DNA-binding motif in regulating substrate recognition and DNA cleavage during the NER process. Single replacements of the conserved Lys141, Lys145, Lys151, Lys179, Lys204 and Arg207 residues with either glycine or glutamate generated XPA mutants that retain overall DNA-repair proficiency, despite the fact that most of these substitutions suppressed binding to double-stranded or single-stranded DNA fragments. This notable disparity between repair activity and DNA-binding capacity revealed that the function of XPA protein during assembly of the excision complex is not coincident with its tendency to associate with linear DNA molecules in reconstituted *in vitro* systems. A subsequent search for mutations in the DNA-binding cleft that more strongly affect DNA repair led to the identification of a double mutant (K141E K179E) characterized by the same low excision capacity that has been associated with severe manifestations of the XP syndrome. A substantial loss of repair proficiency was obtained by mutating positions 141 and 179 simultaneously. All other combinations of double mutants throughout the positively charged DNA-binding surface conferred more moderate effects, indicating a crucial role for Lys141 and Lys179. Also, the repair deficiency was dependent on the insertion of a negatively charged residue in at least one of these two positions, implying that the loss of activity is partly due to electrostatic repulsion between the protein and the DNA backbone.

The conformation of DNA in NER intermediates is likely to deviate from the canonical Watson-Crick geometry. First, different factors (p127–p48 and XPC) that operate upstream of XPA in the repair pathway induce site-specific DNA bends[37,38]. Second, local DNA melting by TFIIH, another subunit that acts upstream of XPA, introduces double-stranded DNA–to–single-stranded DNA transitions on either side of a partially unwound bubble of 20–25 nt[11,39]. Third, the paradigm of eukaryotic transcription shows that the assembly of multicomponent factors on DNA involves, in addition to helix unwinding, changes in the direction of the helical axis, resulting in sharp backbone kinks[31]. To test the affinity of XPA protein for such unusual DNA structures, we used Y-shaped junctions to mimic helical transitions[40] as well as four-way junctions to produce sharp backbone kinks[41]. In a direct comparison between these substrates, XPA protein showed a strong preference for four-way structures over transition molecules and linear double-stranded or single-stranded DNA. We then found that all repair-proficient single or double mutants bind four-way DNA junctions to the same extent as the wild-type control. Even the repair-deficient K141E K179E tandem mutant retains an affinity for four-way junctions identical to that of wild-type XPA. However, the interaction of this tandem mutant with four-way junctions generates aberrant nucleoprotein complexes that migrate in nondenaturing gels with higher electrophoretic mobility than their wild-type counterparts. Photo–cross-linking experiments showed that the subtle molecular defect underlying the formation of such abnormal complexes resides with the inability of the tandem mutant to undergo close contacts with the kinked junction region of four-way DNA. Moreover, unlike the complexes containing wild-type protein, the aberrant nucleoprotein products generated by the mutant are defective in the recruitment of the XPF–ERCC1 endonuclease. These results indicate that the assembly of productive excision intermediates, which include XPF–ERCC1, is dependent on the proper interaction of XPA protein with a narrow bending angle in the DNA substrate.

A role of XPA protein has been postulated during the recognition or verification of DNA damage[1,16,18,29], but it has previously been unclear how a single repair factor might acquire an affinity for all DNA lesions that are processed by the versatile NER system. It has been noted that the general structural feature of DNA carrying bulky adducts is an enhancement of its local conformational flexibility[42]. Thus, we propose that Lys141 and Lys179, located in a concave surface of XPA protein at the edge of the DNA-binding cleft, serve to monitor the increased deformability that is inherent to damaged sites. In analogy with other known factors that have an affinity for kinked DNA[43,44], Lys141 and Lys179 seem to mediate an interaction with the nucleic acid backbone at the site of a sharp kink, where XPA presumably binds as a dimer, whereas other basic residues of the DNA-binding domain mediate non-specific contacts with adjacent linear segments of the substrate. In this model, XPA protein exploits its preference for sharply bent DNA backbones to probe the susceptibility of the DNA helix to be kinked during the assembly of excision complexes.

METHODS

Site-directed mutagenesis. The human *XPA* complementary DNA, together with an N-terminal polyhistidine tag, was subcloned from pET15b-XPA vector[29] into pcDNA3.1 (Invitrogen) using the restriction enzymes XbaI and XhoI. Mutagenesis of *XPA* in plasmids pET15b-XPA and pcXPA was carried out with the QuikChange site-directed mutagenesis kit (Stratagene). The forward and reverse primers are listed in **Supplementary Table 1** online. Tandem mutants were constructed by sequential mutagenesis cycles using appropriately modified primers. The resulting clones were sequenced (Microsynth) to exclude accidental mutations introduced elsewhere in the complementary DNA.

Host-cell reactivation assay. Simian virus 40–transformed human XP-A fibroblasts (GM04312) were from the Coriell Cell Repository. These cells were grown in Dulbecco's modified Eagle's medium (Gibco), supplemented with 10% (v/v) FBS, penicillin G (100 units ml^{-1}) and streptomycin (100 μg ml^{-1}), in a 5% CO_2 humidified incubator. The pGL3 and phRL-TK vectors expressing *Photinus pyralis* (firefly) and *Renilla* luciferase, respectively, were from Promega. The pGL3 vector was UV-irradiated (254 nm, 1,000 J m^{-2}) at a concentration of 1 mg ml^{-1} in 10 mM Tris-HCl (pH 8.0) and 1 mM EDTA. XP-A cells were transfected in a six-well plate at a confluence of 95% using Lipofectamine Plus (Invitrogen). Each transfection mixture contained 0.9 μg pGL3 (UV-irradiated), 0.1 μg phRL-TK (unirradiated) and 0.3 μg pcDNA3.1 or pcXPA. After a 4-h incubation, the transfection reagents were replaced by medium. Unless otherwise indicated, the cells were lysed after another 15 h to measure firefly and *Renilla* luciferase activity using the Dual-Glo assay system (Promega) on a microtiter plate luminometer (Dynex). All results (mean values of at least five measurements) were normalized by calculating the ratios between firefly and *Renilla* luciferase activity.

Proteins. The pET15b-XPA vector was used to express the human XPA protein in *E. coli* strain BL21(DE3)pLysS. Polyhistidine-tagged proteins were purified through a Ni^{2+} column (Qiagen) as described in ref. 29. Chromatographic fractions were analyzed using a mouse monoclonal antibody raised against recombinant human XPA (NeoMarkers). The samples containing XPA protein were pooled, dialyzed against buffer A (25 mM Tris-HCl (pH 8.0), 100 mM NaCl, 10% (v/v) glycerol, 10 mM $NaHSO_3$, 1 mM dithiothreitol and 0.1 mM phenylmethane sulfonyl fluoride) and loaded onto a 5-ml heparin column (Amersham) at a flow rate of 0.5 ml min^{-1}. After washing with buffer A, the column was eluted with a gradient of NaCl (100–800 mM). The samples containing XPA protein, eluting at 500–600 mM NaCl, were dialyzed against buffer A and loaded onto a 1-ml Resource Q column (Amersham) at a flow rate of 0.2 ml min^{-1}. The column was washed with buffer A and eluted with a gradient of NaCl (0.1–1.0 M). Fractions containing XPA, eluting around 800 mM NaCl, were pooled, dialyzed and supplemented with glycerol to a concentration of 25% (v/v) before freezing at –80 °C. Protein concentration was determined using the Bio-Rad protein assay reagent.

Electrophoretic mobility shift assays. Synthetic DNA oligomers were purchased from Microsynth. The 20-mer oligonucleotide 5′-CCTCTCTCTGGTCT TCTTCT-3′ containing a single d(GpG) cisplatin cross-link[45] was annealed to 5′-AGAAGAAGACCAGAGAGAGG-3′. Y-shaped substrates and four-way DNA junctions were prepared by annealing appropriate oligonucleotides as described in ref. 46. Undamaged homoduplex 43-mers and 76-mers were constructed by annealing complementary oligonucleotides of the respective lengths. All hybridizations were performed in 50 mM Tris-HCl (pH 7.4), 10 mM $MgCl_2$ and 1 mM dithiothreitol by heating at 95 °C for 10 min, then slow-cooling (3 h at 25 °C). EMSAs (reactions of 40 μl) were performed by incubating, at 20 °C for 30 min, ^{32}P-labeled DNA substrate (0.56 pmol), unlabeled homoduplex competitor DNA (19-mer, 1 pmol) and the indicated amounts of XPA in buffer B (25 mM HEPES-KOH (pH 8.3), 30 mM KCl, 4 mM $MgCl_2$, 1 mM EDTA, 0.9 mM DTT, 45 μg ml^{-1} BSA and 10% (v/v) glycerol). After the addition of gel-loading buffer (4 μl) containing 100 mM Tris-HCl (pH 8.3), 10% (v/v) glycerol and 0.05% (w/v) orange G, the extent of binding was determined on 7% nondenaturing polyacrylamide gels. Electrophoresis was performed at 1.5 mA cm^{-1} for 20–40 min at room temperature. Gels were dried and subjected to autoradiography.

Circular dichroism spectra. XPA samples (0.4 mg ml^{-1}) were dialyzed against 20 mM phosphate buffer. Far-UV spectra were determined at 20 °C with a JASCO J-715 spectrometer using a 1-mm quartz cell. Each spectrum was recorded five times and averaged. The data were normalized to protein concentrations measured by the absorbance at 280 nm.

Photo–cross-linking assay. Reactions were initiated by incubating photoreactive probes[47] (0.56 pmol) for 5 min at 20 °C in 25 mM HEPES-KOH (pH 8.3), 4 mM $MgCl_2$, 10% (v/v) glycerol, 45 μg ml^{-1} BSA and 2 mM EDTA with the concentrations of XPA protein indicated in **Figure 5**. Cross-linking was induced by exposure to UV light (100 sec) using the UVG-11 source from UVP. The samples were dissolved in gel-loading buffer (60 mM Tris-HCl (pH 6.8), 2% (v/v) glycerol, 2% (w/v) sodium dodecyl sulfate, 2.5 mM dithiothreitol, 2% (v/v) 2-mercaptoethanol and 0.005% (w/v) bromophenol blue). After boiling for 5 min, the cross-linked products were resolved on denaturing 15% polyacrylamide gels and visualized by autoradiography.

Pull-down assays. The GST-XPA fusions were constructed by inserting the *XPA* complementary DNA into the pGEX-4T-1 vector (Amersham) using the EcoRI and XhoI restrictions. The resulting clones were expressed in *E. coli* strain BL21(DE3)pLysS. GST fusion proteins (10 nM) were incubated at 4 °C for 30 min with glutathione-Sepharose beads (25 μl) in 500 μl washing buffer (50 mM Tris-HCl (pH 8.0), 1 mM EDTA, 1 mM dithriothreitol, 10% (v/v) glycerol, 0.5% (v/v) Nonidet P-40, 150 mM NaCl and 200 μg ml^{-1} BSA) containing 0.5% (w/v) nonfat milk. Each sample was washed three times and incubated on a rocker in 500 μl buffer B with 10 nM polyhistidine-tagged ERCC1-XPF or XPA protein. After 20 min at room temperature, the beads were washed five times, resuspended in gel-loading buffer, boiled for 5 min and analyzed on denaturing 15% polyacrylamide gels. The presence of tagged ERCC1 or XPA was probed by western blotting using polyhistidine antibodies (Santa Cruz Biotechnology).

Note: Supplementary information is available on the Nature Structural & Molecular Biology website.

ACKNOWLEDGMENTS

We thank M. Vitanescu for excellent technical assistance, J. Kaspàrkovà (Academy of Sciences of the Czech Republic) for the gift of cisplatin-modified oligonucleotides and O. Schärer (State University of New York, Stony Brook) for the gift of XPF–ERCC1. This work was supported by Swiss National Science Foundation grant 3100A-101747.

COMPETING INTERESTS STATEMENT

The authors declare that they have no competing financial interests.

Published online at http://www.nature.com/nsmb/
Reprints and permissions information is available online at http://npg.nature.com/reprintsandpermissions/

1. Sancar, A. DNA excision repair. *Annu. Rev. Biochem.* **65**, 43–81 (1996).
2. Wood, R.D. Nucleotide excision repair in mammalian cells. *J. Biol. Chem.* **272**, 23465–23468 (1997).
3. De Laat, W.L., Jaspers, N.G. & Hoeijmakers, J.H. Molecular mechanism of nucleotide excision repair. *Genes Dev.* **13**, 768–785 (1999).
4. Mitchell, D.L. The induction and repair of lesions produced by the photolysis of (6–4) photoproducts in normal and UV-hypersensitive human cells. *Mutat. Res.* **194**, 227–237 (1988).
5. Reardon, J.T. & Sancar, A. Recognition and repair of the cyclobutane thymine dimer, a major cause of skin cancers, by the human excision nuclease. *Genes Dev.* **17**, 2539–2551 (2003).
6. Friedberg, E.C., Walker, G.C. & Siede, W. *DNA Repair and Mutagenesis* (ASM Press, Washington, DC, USA, 1995).
7. Kraemer, K.H., Lee, M.M. & Scotto, J. DNA repair protects against cutaneous and internal neoplasia: evidence from xeroderma pigmentosum. *Carcinogenesis* **5**, 511–514 (1984).
8. States, J.C., McDuffie, E.R., Myrand, S.P., McDowell, M. & Cleaver, J.E. Distribution of mutations in the human xeroderma pigementosum group A gene and their relationships to the functional regions of the DNA damage recognition protein. *Hum. Mutat.* **12**, 103–113 (1998).
9. Cleaver, J.E., Thompson, L.H., Richardson, A.S. & States, J.C. A summary of mutations in the UV-sensitive disorders: xeroderma pigementosum, Cockayne syndrome, and trichothiodystrophy. *Hum. Mutat.* **14**, 9–22 (1999).

10. Huang, J.C., Svoboda, D., Reardon, J.T. & Sancar, A. Human nucleotide excision nuclease removes thymine dimers from DNA by incising the 22nd phosphodiester bond 5′ and the 6th phosphodiester bond 3′ to the photodimer. *Proc. Natl. Acad. Sci. USA* **89**, 3664–3668 (1992).
11. Evans, E., Fellows, J., Coffer, A. & Wood, R.D. Open complex formation around a lesion during nucleotide excision repair provides a structure for cleavage by human XPG protein. *EMBO J.* **16**, 625–638 (1997).
12. Aboussekhra, A. *et al.* Mammalian DNA nucleotide excision repair reconstituted with purified protein components. *Cell* **80**, 859–868 (1995).
13. Mellon, I., Spivak, G. & Hanawalt, P.C. Selective removal of transcription-blocking DNA damage from the transcribed strand of the mammalian DHFR gene. *Cell* **51**, 241–249 (1987).
14. Friedberg, E.C. DNA damage and repair. *Nature* **421**, 436–440 (2003).
15. Mu, D. *et al.* Reconstitution of human DNA repair excision nuclease in a highly defined system. *J. Biol. Chem.* **270**, 2415–2418 (1995).
16. Sugasawa, K. *et al.* Xeroderma pigmentosum group C protein complex is the initiator of global genome nucleotide excision repair. *Mol. Cell* **2**, 223–232 (1998).
17. Araújo, S.J. *et al.* Nucleotide excision repair of DNA with recombinant human proteins: definition of the minimal set of factors, active forms of TFIIH, and modulation by CAK. *Genes Dev.* **14**, 349–359 (2000).
18. Volker, M. *et al.* Sequential assembly of the nucleotide excision repair factors in vivo. *Mol. Cell* **8**, 213–224 (2001).
19. Yang, Z.G., Liu, Y., Mao, L.Y., Zhang, J.-T. & Zou, Y. Dimerization of human XPA and formation of XPA_2-RPA protein complex. *Biochemistry* **41**, 13012–13020 (2002).
20. He, Z., Henricksen, L.A., Wold, M.S. & Ingles, C.J. RPA involvement in the damage-recognition and incision steps of nucleotide excision repair. *Nature* **374**, 566–569 (1995).
21. Li, L., Lu, X., Peterson, C.A. & Legerski, R.J. An interaction between the DNA repair factor XPA and replication protein A appears essential for nucleotide excision repair. *Mol. Cell. Biol.* **15**, 5396–5402 (1995).
22. Park, C.H., Mu, D., Reardon, J.T. & Sancar, A. The general transcription-repair factor TFIIH is recruited to the excision repair complex by the XPA protein independent of the TFIIE transcription factor. *J. Biol. Chem.* **270**, 4896–4902 (1995).
23. Kuraoka, I. *et al.* Identification of a damaged-DNA binding domain of the XPA protein. *Mutat. Res.* **362**, 87–95 (1996).
24. Cleaver, J.E. & States, J.C. The DNA damage-recognition problem in human and other eukaryotic cells: the XPA damage binding protein. *Biochem. J.* **328**, 1–12 (1997).
25. Ikegami, T. *et al.* Solution structure of the DNA-and RPA-binding domain of the human repair factor XPA. *Nat. Struct. Biol.* **5**, 701–706 (1998).
26. Buchko, G.W. *et al.* DNA-XPA interactions: a ^{31}P NMR and molecular modeling study of dCCAATAACC association with the minimal DNA-binding domain (M98–F219) of the nucleotide excision repair protein XPA. *Nucleic Acids Res.* **29**, 2635–2643 (2001).
27. Carreau, M. *et al.* Development of a new easy complementation assay for DNA repair deficient human syndromes using cloned repair genes. *Carcinogenesis* **16**, 1003–1009 (1995).
28. Mellon, I., Hock, T., Reid, R., Porter, P.C. & States, J.C. Polymorphisms in the human xeroderma pigmentosum group A gene and their impact on cell survival and nucleotide excision repair. *DNA Repair (Amst.)* **1**, 531–546 (2002).
29. Jones, C.J. & Wood, R.D. Preferential binding of the xeroderma pigmentosum group A complementing protein to damaged DNA. *Biochemistry* **32**, 12096–12104 (1993).
30. You, J.S., Wang, M. & Lee, S.H. Biochemical analysis of the damage recognition process in nucleotide excision repair. *J. Biol. Chem.* **278**, 7476–7485 (2003).
31. Werner, M.H., Gronenborn, A.M. & Clore, G.M. Intercalation, DNA kinking, and the control of transcription. *Science* **271**, 778–784 (1996).
32. Rost, B., Yachdav, G. & Liu, J. The PredictProtein server. *Nucleic Acids Res.* **32**, W321–W326 (2004).
33. Riedl, T., Hanaoka, F. & Egly, J.M. The comings and goings of nucleotide excision repair factors on damaged DNA. *EMBO J.* **22**, 5293–5303 (2003).
34. Enzlin, J.H. & Schärer, O.D. The active site of the DNA repair endonuclease XPF-ERCC1 forms a highly conserved nuclease motif. *EMBO J.* **21**, 2045–2053 (2002).
35. McDowell, M.L., Nguyen, T. & Cleaver, J.E. A single-site mutation in the XPAC gene alters photoproduct recognition. *Mutagenesis* **8**, 155–161 (1993).
36. Kobayashi, T. *et al.* Mutational analysis of a function of xeroderma pigmentosum group A (XPA) protein in strand specific repair. *Nucleic Acids Res.* **26**, 4662–4668 (1998).
37. Fujiwara, Y. *et al.* Characterization of DNA recognition by the human UV-damaged DNA-binding protein. *J. Biol. Chem.* **274**, 20027–20033 (1999).
38. Janicijevic, A. *et al.* DNA bending by the human damage recognition complex XPC-HR23B. *DNA Repair (Amst.)* **2**, 325–336 (2003).
39. Mu, D., Wakasugi, M., Hsu, D.S. & Sancar, A. Characterization of reaction intermediates of human excision repair nuclease. *J. Biol. Chem.* **272**, 28971–28979 (1997).
40. O'Donovan, A., Davies, A.A., Moggs, J.G., West, S.C. & Wood, R. XPG endonuclease makes the 3′ incision in human DNA nucleotide excision repair. *Nature* **371**, 432–435 (1994).
41. Ortiz-Lombardia, M. *et al.* Crystal structure of a DNA Holliday junction. *Nat. Struct. Biol.* **6**, 913–917 (1999).
42. Isaacs, R.J. & Spielmann, H.P. A model for initial DNA lesion recognition by NER and MMR based on local conformational flexibility. *DNA Repair (Amst.)* **3**, 455–464 (2004).
43. Weir, H.M. *et al.* Structure of the HMG box motif in the B-domain of HMG1. *EMBO J.* **12**, 1311–1319 (1993).
44. Read, C.M., Cary, P.D., Crane-Robinson, C., Driscoll, P.C. & Norman, D.G. Solution structure of a DNA-binding domain from HMG1. *Nucleic Acids Res.* **21**, 3427–3436 (1993).
45. Kasparkova, J., Mellish, K.J., Qu, Y. & Brabec, V. Site-specific d(GpG) intrastrand cross-links formed by dinuclear platinum complexes. Bending and NMR studies. *Biochemistry* **35**, 16705–16713 (1996).
46. Missura, M. *et al.* Double-check probing of DNA binding and unwinding by XPA-RPA: an architectural function in DNA repair. *EMBO J.* **20**, 3554–3564 (2001).
47. Dip, R. & Naegeli, H. Binding of the DNA-dependent protein kinase catalytic subunit to Holliday junctions. *Biochem. J.* **381**, 165–174 (2004).
48. Ford, J.M. & Hanawalt, P.C. Li-Fraumeni syndrome fibroblasts homozygous for p53 mutations are deficient in global DNA repair but exhibit normal transcription-coupled repair and enhanced UV resistance. *Proc. Natl. Acad. Sci. USA* **92**, 8876–8880 (1995).

Recognition of helical kinks by xeroderma pigmentosum group A protein triggers DNA excision repair

Ulrike Camenisch, Ramiro Dip, Sylvie Briand Schumacher, Benjamin Schuler & Hanspeter Naegeli

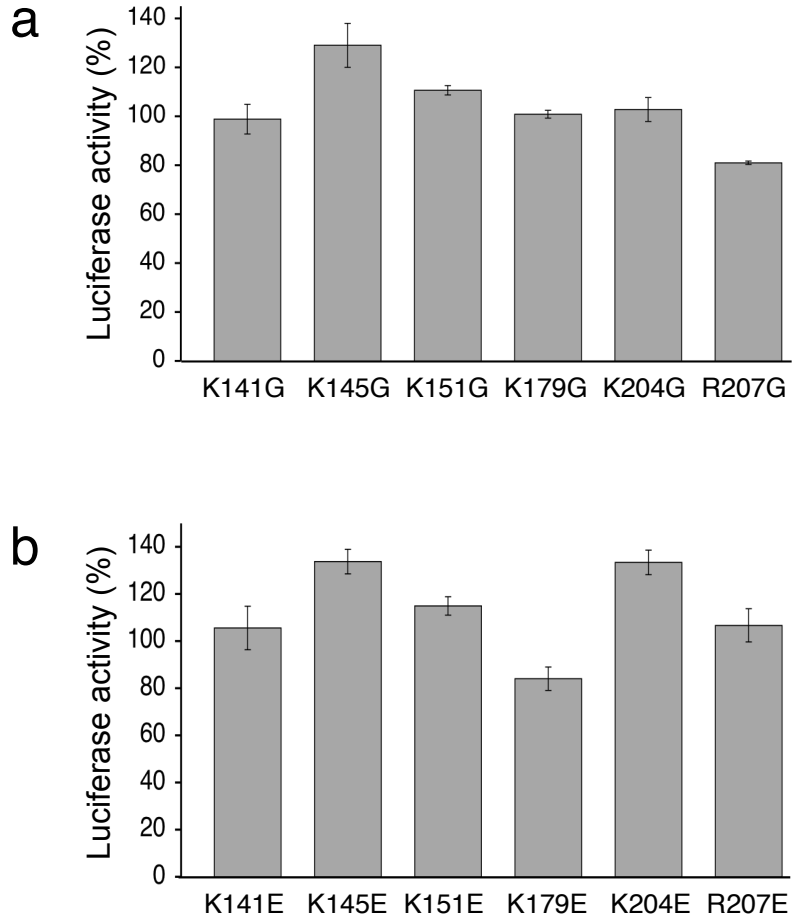

Supplementary Figure 1. Screening of single XPA mutants by host cell reactivation assay in human fibroblasts. (**a**) Repair proficiency of glycine mutants in the putative DNA binding cleft of human XPA protein. (**b**) Repair proficiency of single glutamic acid mutants in the DNA binding cleft. Results are expressed as the percentage of wild-type complementation after deduction of background luciferase activity obtained with empty vector.

Recognition of helical kinks by xeroderma pigmentosum group A protein triggers DNA excision repair

Ulrike Camenisch, Ramiro Dip, Sylvie Briand Schumacher, Benjamin Schuler & Hanspeter Naegeli

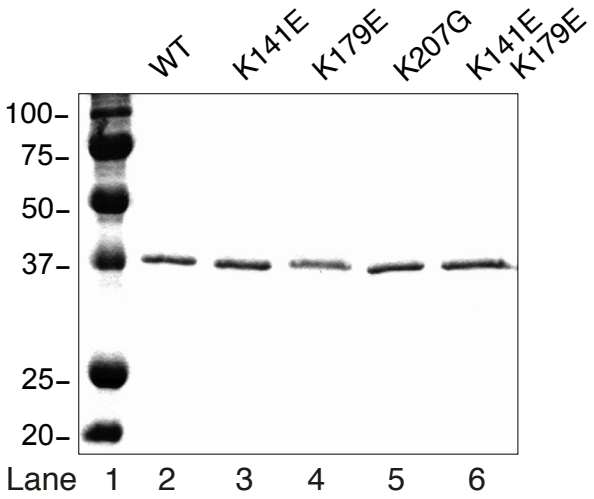

Supplementary Figure 2. Denaturing polyacrylamide gel demonstrating the purity of wild-type (lane 2) and mutant XPA proteins (lanes 3-6). Lane 1: molecular weight markers.

Recognition of helical kinks by xeroderma pigmentosum group A protein triggers DNA excision repair

Ulrike Camenisch, Ramiro Dip, Sylvie Briand Schumacher, Benjamin Schuler & Hanspeter Naegeli

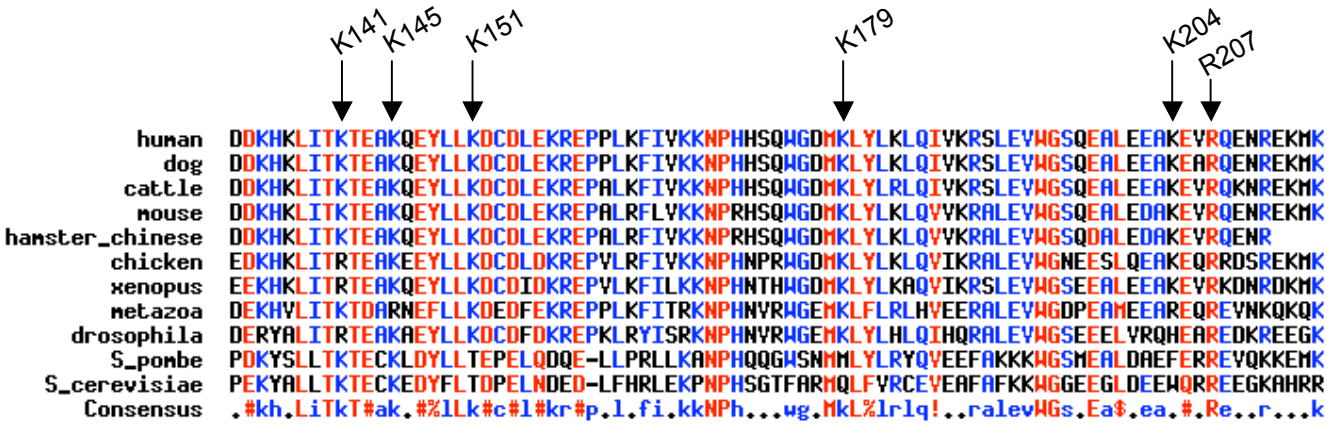

Supplementary Figure 3. Sequence comparison between eukaryotic XPA homologs. The positions of basic amino acids on the surface of the presumed DNA binding cleft are indicated by the arrows.

Recognition of helical kinks by xeroderma pigmentosum group A protein triggers DNA excision repair

Ulrike Camenisch, Ramiro Dip, Sylvie Briand Schumacher, Benjamin Schuler
& Hanspeter Naegeli

Supplementary Table 1. Forward and reverse primers used for site-directed mutagenesis. The mutated nucleotides are underlined.

Mutation	Oligonucleotide primer sequences
K135E K137E	5'-GCAGAGATGCTGATGAT**G**AACAC**G**AGCTTATAACCAAAACAGAGGC-3' 5'-GCCTCTGTTTTGGTTATAAGCT**C**GTGTT**C**ATCATCAGCATCTCTGC-3'
K141G	5'-AACACAAGCTTATAACC**GG**AACAGAGGCAAAACAAGAATATC-3' 5'-GATATTCTTGTTTTGCCTCTGTT**CC**GGTTATAAGCTTGTGTT-3'
K141E	5'-CACAAGCTTATAACC**G**AAACAGAGGCAAAACAAGAATATCTTCTG-3' 5'-CAGAAGATATTCTTGTTTTGCCTCTGTTT**C**GGTTATAAGCTTGTG-3'
K141Q	5'-CACAAGCTTATAACC**C**AAACAGAGGCAAAACAAGAATATCTTCTG-3' 5'-CAGAAGATATTCTTGTTTTGCCTCTGTTT**G**GGTTATAAGCTTGTG-3'
K145G	5'-TAACCAAAACAGAGGCA**GG**ACAAGAATATCTTCTGAAAG-3' 5'-CTTTCAGAAGATATTCTTGT**CC**TGCCTCTGTTTTGGTTA-3'
K145E	5'-GCTTATAACCGAAACAGAGGCA**G**AACAAGAATATCTTCTG-3' 5'-CAGAAGATATTCTTGTT**C**TGCCTCTGTTTCGGTTATAAGC-3'
K151G	5'-ACAGAGGCAAAACAAGAATATCTTCTG**GG**AGACTGTGATTTAG-3' 5'-CTAAATCACAGTCT**CC**CAGAAGATATTCTTGTTTTGCCTCTGT-3'
K151E	5'-GGCAAAACAAGAATATCTTCTG**G**AAGACTGTGATTTAGAAAAAAG-3' 5'-CTTTTTTCTAAATCACAGTCTT**C**CAGAAGATATTCTTGTTTTGCC-3'
K157E	5'-CTGAAAGACTGTGATTTAGAA**G**AAAGAGAGCCACCTC-3' 5'-GAGGTGGCTCTCTTT**C**TTCTAAATCACAGTCTTTCAG-3'

K158E	5'-CTGAAAGACTGTGATTTAGAAAAA**GA**AGAGCCACCTCTTAAATTTATTG-3' 5'-CAATAAATTTAAGAGGTGGCTCT**TC**TTTTTCTAAATCACAGTCTTTCAG-3'
K167E K168E	5'-CCACCTCTTAAATTTATTGTG**G**AG**G**AGAATCCACATCATTCACAATGG-3' 5'-CCATTGTGAATGATGTGGATTCT**C**CT**C**CACAATAAATTTAAGAGGTGG-3'
K179G	5'-ATTCACAATGGGGTGATATG**GG**ACTCTACTTAAAGTTACAG-3' 5'-CTGTAACTTTAAGTAGAGT**CC**CATATCACCCCATTGTGAAT-3'
K179E	5'-CACAATGGGGTGATATG**G**AACTCTACTTAAAGTTACAGATTG-3' 5'-CAATCTGTAACTTTAAGTAGAGTT**C**CATATCACCCCATTGTG-3'
K179Q	5'-CACAATGGGGTGATATG**C**AACTCTACTTAAAGTTACAGATTG-3' 5'-CAATCTGTAACTTTAAGTAGAGTT**G**CATATCACCCCATTGTG-3'
K204G	5'-AGAAGCATTAGAAGAAGCA**GG**GGAAGTCCGACAGG-3' 5'-CCTGTCGGACTTCC**CC**TGCTTCTTCTAATGCTTCT-3'
K204E	5'-GTCAAGAAGCATTAGAAGAAGCA**G**AGGAAGTCCGACAGG-3' 5'-CCTGTCGGACTTCCT**C**TGCTTCTTCTAATGCTTCTTGAC-3'
R207G	5'-AAGAAGCAAAGGAAGTC**G**GACAGGAAAACCGAG-3' 5'-CTCGGTTTTCCTGTC**C**GACTTCCTTTGCTTCTT-3'
R207E	5'-GCATTAGAAGAAGCAAAGGAAGTC**GA**ACAGGAAAACCGAGAAAAAATG-3' 5'-CATTTTTTCTCGGTTTTCCTGT**TC**GACTTCCTTTGCTTCTTCTAATGC-3'
R207stop	5'-GCATTAGAAGAAGCAAAGGAAGTC**T**GACAGGAAAACCGAGAAAAAATG-3' 5'-CATTTTTTCTCGGTTTTCCTGTC**G**GACTTCCTTTGCTTCTTCTAATGC-3'
R228Q	5'-GTAAAAGAATTGCGGC**A**AGCAGTAAGAAGCAGCG-3' 5'-CGCTGCTTCTTACTGCT**T**GCCGCAATTCTTTTAC-3'